Proceedings of the 2002 IEEE
International Conference on Robotics & Automation
Washington, DC • May 2002

Sensor-Based Exploration for Convex Bodies: A New Roadmap for a Convex-shaped Robot

Ji Yeong Lee Howie Choset
Carnegie Mellon University
jiyeongl,choset+@andrew.cmu.edu

Abstract

We present a new algorithm that enables a convex shaped robot to explore an unknown planar workspace, i.e., an unknown configuration space diffeomorphic to $SE(2)$. This new algorithm is based on a new roadmap called the *convex hierarchical generalized Voronoi graph* (convex-HGVG), which is the central contribution of this paper. Since this roadmap is defined in terms of workspace distance information which is within line of sight of the convex body, we can use this roadmap to direct the robot to explore the unknown space. The challenge in defining the roadmap is that $SE(2)$, with holes removed from it, does not have, in general, a one-dimensional retract. Therefore, we decompose the punctured $SE(2)$ into contractible regions in which we define convex generalized Voronoi graphs (convex-GVG) and then connect these graphs with additional structures called R-edges. The convex-GVG edges and the R-edges together form the convex-HGVG. We show that the convex-HGVG is indeed a roadmap and then we demonstrate the control laws that a robot can invoke that incrementally constructs the roadmap.

1 Introduction

Sensor based planning is necessary for the realistic deployment of robots into unknown spaces. Many geometric challenges face this problem: which information does the robot require? How does the planner use this information to move about its environment to map it? How does the planner respect the physical dimensions of the robot? Our goal is to develop a provably complete and reactive planner that maps an unknown region by invoking a simple sequence of control laws (i.e., reactive behaviors) and arbitrating among them at key salient points.

In the past, most provably complete sensor based planners [10, 8, 2] addressed many of the challenges of sensor based planning but were limited to robots modeled as point robots operating in the plane. Recent work of Yap [5] and Choset [4, 7] considered a robot that can be modeled as a line segment or a rod, which has three-degrees of freedom in the plane and five degrees in three dimensions. This paper takes the next step in defining a roadmap for a convex body. Our sensor-based approach is derived from a new roadmap of the convex body's three-dimensional configuration space $\mathbb{R}^2 \times S^1$ termed the *convex hierarchical generalized Voronoi graph* (convex-HGVG) for the convex bodies. A planner uses a roadmap to plan a path between two configurations in three steps: plan a path onto the roadmap (accessibility); plan a path along the roadmap (connectivity); and plan a path from the roadmap (departability) [1].

If the robot incrementally constructs the convex-HGVG, then in essence it has explored the unknown space because the planner can use the roadmap to plan future excursions. Since the convex-HGVG is a collection of edges and nodes, its definition naturally induces a sequence of control laws (one for the edges and one for homing onto edges) and arbitration schemes (to select edges at its nodes), which results in a reactive hybrid system that explores an unknown space.

The primary challenge in defining a roadmap for a convex body in $\mathbb{R}^2 \times S^1$ is that $\mathbb{R}^2 \times S^1$ with functions (from configuration space obstacles) is not contractible. This means that we cannot define a retraction on the convex body's configuration space as we could with the *generalized Voronoi diagram* (GVD) [9].

The outline of the paper is as follows: Section 2 describes the prior works related to this paper. Section 3 defines the components of convex-HGVG and proves that this roadmap has all desired properties, most importantly, the convex-HGVG forms a connected set. Section 4 presents a incremental construction method for the convex-HGVG. Section 5 presents some simulation results and section 6 summerizes the results and discusses the future directions.

2 Relation to Prior Work

Recall that the GVD is the set of points in the plane equidistant to two obstacles, i.e., $GVD = \bigcup\{x \in \mathbb{R}^2 : 0 < d_i(x) = d_j(x) \leq d_h(x) \ \ \forall h\}$ where $d_i(x)$ measures the distance to an obstacle C_i. Yap shows that the GVD is the image of a retraction Im is the GVD itself. The GVD edges terminate and intersect at nodes called *meet points*

which are the set of points equidistant to three and more obstacles (See Figure 1),

Choset and Burdick (as well as others) extend the GVD into three dimensions by defining the *generalized Voronoi graph* (GVG) which is the set of points equidistant to three obstacles. The GVG, by itself, was not connected and thus additional structures, called higher order GVG's were introduced yielding a connected roadmap called the hierarchical generalized Voronoi graph (HGVG) [3].

Next, Choset et. al. defined a roadmap for rod-shaped robots operating in the plane. This robot has three degrees of freedom and hence we define a rod-GVG edge as the set of points equidistant to three obstacles. Distance had to be re-defined as $D_i(q) = \min_{r \in R(q), c \in C_i} \|r - c\|$ where $q = [x, y, \theta]^T \in SE(2)$ is the configuration of the rod and $R(q)$ is the set of points that the rod occupies when it is located at configuration q.

Alas, like the point-GVG, the rod-GVG is not connected, so we defined additional structures called R-edges which are based on the point-GVG. Just as the rod-GVG edges are the "SE(2)-generalization" of point-GVG nodes (meet points), the R-edges are the "SE(2)-equivalent" to point-GVG edges. The R-edges are the set of rod configurations that are tangent to the two-way equidistant point-GVG edges. The collection of the R-edges and rod-GVG edges form the rod-HGVG. (See Figure 2). What is interesting here is that we are able to use information about the topology of the work space to infer a topological property of the rod's configuration space.

Since the convex body has three degrees of freedom as well, it is natural to define a convex-GVG edge as the set of points equidistant to three obstacles, as we have done with the rod. Ong and Keerthi have a similar definition for a convex-GVG edge [6]. Just like the rod-GVG, the convex-GVG (the collection of convex-GVG edges) will not form a connected set, in general. Ong and Keerthi have developed some heuristics to connect the convex-GVG edges but they lack provable guarantees. The real innovation presented in this paper is the definition of the R-edges for convex bodies (Figure 3). This structure goes beyond heuristics and allow us to rigorously connect the roadmap, i.e, connect convex-GVG edges in a provably complete manner.

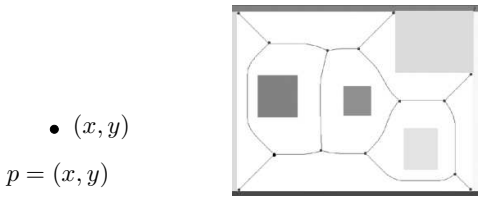

Figure 1: Point-GVG or the generalized Voronoi diagram, which is the set of points equidistant to two obstacles.

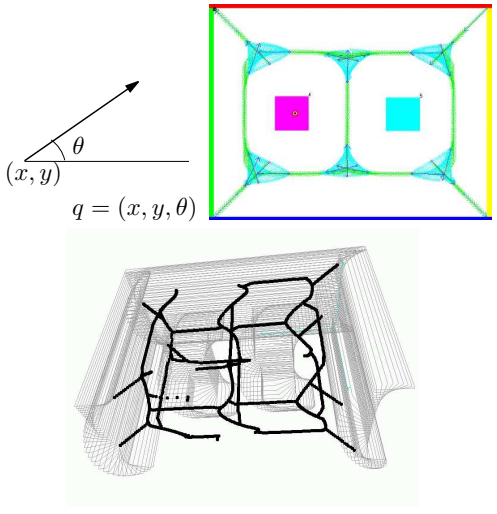

Figure 2: Placements of the rod along the rod-HGVG and the configuration space view of the rod-HGVG

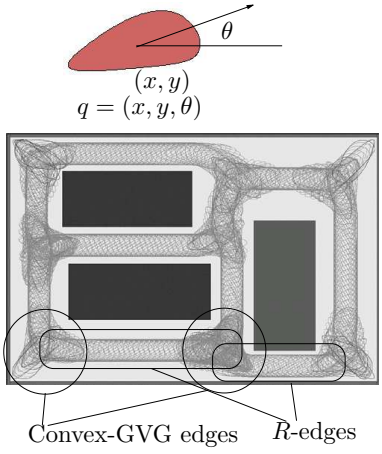

Figure 3: Placements of a convex-shaped robot along the convex-HGVG.

3 Convex Hierarchical Generalized Voronoi Graph

The convex body moving in the plane has three degrees-of-freedom whose configuration is represented as $q = (x, y, \theta)^T$. Let $R(q) \subset \mathbb{R}^2$ be the set of points that the convex body occupies in the plane when it is located at q. Then, the distance between the obstacle C_i and the robot

at q is defined as

$$D_i(q) = \min_{r \in R(q), c \in C_i} \|r - c\|. \quad (1)$$

We use equidistance relationships to define the convex-HGVG. The set of configurations equidistant to two obstacles is

$$CF_{ij} = \{q \in SE(2) : 0 \leq D_i(q) = D_j(q) \leq D_h(q) \forall h \neq i, j \text{ and } \nabla D_i(q) \neq \nabla D_j(q)\}.$$

One could construct the co-dimension one convex-GVD as $\cup_i \cup_j CF_{ij}$.

3.1 Convex-GVG Edge

A convex-GVG edge is the set of configurations equidistant to three obstacles, which is formed by intersecting the above defined two-way equidistant surfaces, i.e., a convex GVG edge equidistant to obstacles C_i, C_j, and C_k is

$$CF_{ijk} = CF_{ij} \cap CF_{jk} \cap CF_{ik}. \quad (2)$$

Definition 1 (Convex Generalized Voronoi Graph) *The **convex-GVG** is the union of convex-GVG edges, i.e., the set of configurations that are three-way equidistant which can be written as*

$$\cup_{i=1}^{i=n-2} \cup_{j=i+1}^{j=n-1} \cup_{k=j+1}^{j=n} CF_{ijk}. \quad (3)$$

Just as we have meet points for the point-GVG, we also have *meet configurations* for the convex GVG which are the configurations equidistant to four or more obstacles; these configurations are the end points of convex-GVG edges. If the convex body is small when compared to the scale of the environment, no convex-GVG meet configurations will exist. With this mind, just like the rod-GVG, the convex-GVG is not necessarily connected, even in the planar case. To produce a connected structure we introduce a new type of *R-edges*.

Accessibility can be shown exactly same way as in the case of the planar rod-HGVG (Choset [4]). That is, the accessibility procedure is a sequence of fixed-orientation gradient ascents of distance function to closest obstacles. It can be proven that the robot reaches a three-way configuration, which is an element of a convex-GVG edge. Also, as in planar rod-HGVG, we define the *junction region* J_{ijk} as a pre-image of a convex-GVG edge under the accessibility function.

3.2 R-Edges: Using Workspace Topology to Infer Configuration Space Topology

Just like the R-edges for the rod-GVG, we use the double equidistant configurations to connect disconnected convex-GVG edges. The set of two-way equidistant configurations

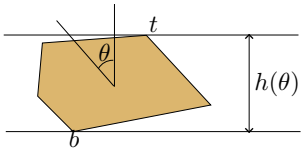

Figure 4: Height function. The points t and b "determine" the height at given orientation.

forms a two-dimensional set, so we have to introduce another constraint. Roughly speaking, since double equidistance is a constraint on position, this additional constraint will be on orientation. For the case of the rod, loosely speaking, there is a natural way to specify the orientation of the rod on the point-GVG edge, which is to make the rod "tangent" a to the point-GVG edge. However, for convex shape, there is no direct sense of tangency. The R-edge definition generalizes this notion of tangency for the convex body.

To generalize this notion of tangency to define an R-edge for a convex body, we use *principal axes* which we derive from the the *height function* which, as its name suggests, measures the height of a set. To picture height, imagine grabbing a convex set at a fixed orientation with a parallel jaw gripper. The distance between the parallel jaws is the height function (Figure 4). More precisely, define n to be the unit vector in a reference direction and θ to be the orientation of the convex body with respect to n. Then, the height $h : S^1 \to \mathbb{R}$ is $\max_{t,b \in A(\theta)}(t - b) \cdot n$, where $A(\theta)$ is the set of the points occupied by a convex set A oriented at θ. We call the two points t and b that determines the height at given orientation as *top* and *bottom* points.

Note that for convex shapes, the height function has a finite number of local minima and we use these minima to define the principal axes[1]. Let $t : S^1 \to \mathbb{R}^2$ and $b : S^1 \to \mathbb{R}^2$ the top and bottom points on a convex set in a body-fixed coordinate frame for a given orientation. Let $\{\theta_i^*\}$ be the set orientations where the height function h obtains minimal values. A *principal axis* v_i is the unit vector that is normal to the vector $(t(\theta_i^*) - b(\theta_i^*))$.

Consider a path that passes between two obstacles C_i and C_j with end points q_k and q_l on CF_{ijk} and CF_{ijl} respectively. This path is a subset of the manifold CF_{ij}. We construct this path such that it has one local minimum of D_i along the path(we know we can do this because the two-way equidistant point-GVG has a unique minimum for distance along each of its edges [3]). Now, we want to consider only such paths for which this local minimum of $D_i(q)$ is locally maximized (See Figure 6). In other words, let Π

[1]Here, we abuse the terminology. In the rest of this paper, the *principal axis* does not mean the usual definition of the term used in dynamics or solid mechanics. Instead, it means some specific orientation in the robot coordinate frame as defined below

be the set of the two-way equidistant path between CF_{ijk} and CF_{ijl} on CF_{ij}, i.e. $\Pi = \{c \in C^0 | c(t) \in CF_{ij}$ for $t \in [0,1]$, and $c(0) \in CF_{ijk}$ and $c(1) \in CF_{ijl}\}$. Let $\Gamma : \Pi \to \mathbb{R}$ be a function such that $\Pi(c) = \min_{q \in c} D_i(q)$. We consider only the paths which attain local maxima of Γ. Note that there will be infinitely many such paths.

We will now restate an equivalent condition which must be satisfied to locally maximize the minimum distance along one of these paths. This condition is: let c_i^* and c_j^* be the pair of closest points in C_i and C_j, i.e., the points in each obstacle where $d(p_i, p_j)$, $p_i \in C_i$, $p_j \in C_j$ is minimized. Let r_i and r_j be the closest points on the robot to C_i and C_j, respectively. Define a configuration m^* where the vector $r_i - r_j$ in the plane is parallel to $c_i^* - c_j^*$ and $D_i(q) = D_j(q)$ (Fig. 7). Note that at this configuration m^*, the robot is located in between two parallel lines, both of which are tangent to the obstacles at c_i^* and c_j^* respectively, and a principal axis is parallel to these parallel lines (See q_2 in Fig.5).

Now to obtain to a specific path that passes through configuration m^*, we define the R-edge as follows:

$$R_{ij} = \{q \in CF_{ij} | \langle c_i - c_j, v_k \rangle = 0 \text{ for some } k\}. \quad (4)$$

where the v_ks are the principal axes of the robot (See Figure 5). Note that under this definition of R-edge, the configuration m^* defined above is contained in R-edge.

The convex robot may have multiple symmetries, and thus multiple principal axes. Therefore there would be more than two R-edges that connect two adjacent convex-GVG edges, as shown in Figures 8 and 9. Here q_1 and q_2 are the two configuration that belong to the disconnected component of CF_{234}. To move from q_1 to q_2, the robot must travel along an R-edge (which contains m_2) to CF_{123} and then, travel back to q_2 along another R-edge (which contains m_1).

3.2.1 Connectivity and Construction of the R-edge: In this section, we prove the connectivity of the convex-HGVG, which can be stated formally as follows.

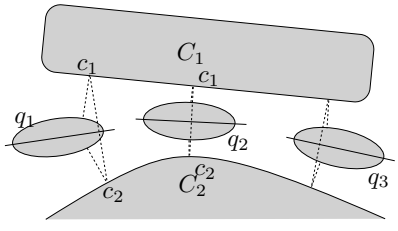

Figure 5: Some placements of the robot in a R-edge R_{12}. All the configuration shown in the figure are (i) equidistant to C_1 and C_2 and (ii) $c_1 - c_2$ is normal to the principal axis of the robot.

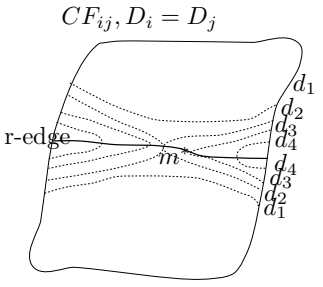

Figure 6: The two-equidistant face CF_{ij} in configuration space. The dotted lines represent the set of the configurations whose distances are constant with $d_1 < d_2 < d_3 < d_4$. To maximize the minimum distance along the path, the path must pass through the configuration m^*, where exactly two constant distant curves meet. Then, along any path on CF_{ij}, the distance will increase in both direction as the robot follows the path away from the point m^*. Essentially, m^* is a saddle point of the distance function on CF_{ij}.

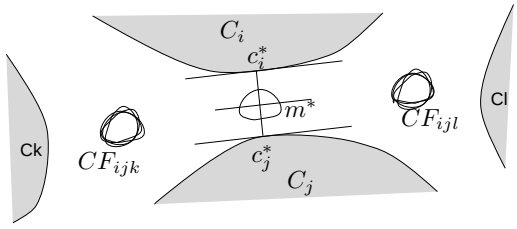

Figure 7: Any path between CF_{ijk} and CF_{ijl} must "pass through" the line segment $c_i^* c_j^*$, where the distance between the two obstacles are determined. To maximize the minimum distance along the path, the robot must align its principal axis to the tangent of the obstacles at c_i^* (and c_j^*). Note that R-edge is defined such that it contains such a configuration.

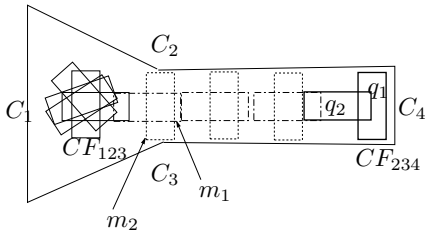

Figure 8: In this example, q_1 and q_2 both belong to the GVG edge CF_{234} but belong the the components that are not connected to each other. To form a connected roadmap, we need both of the r-edges represented dotted lines and dashed lines, which corresponds to each of the principal axes of the robot. m_1 and m_2 are the configuration along each component where the distance to the two closest obstacles is locally minimized.

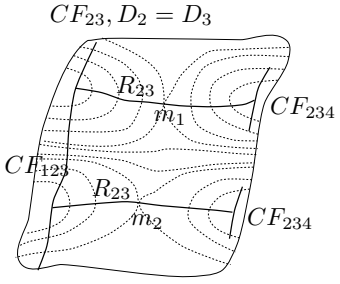

Figure 9: The (rough) representation of the environment in Fig. 8 in configuration space. The two R-edge component connects the two disconnected components of the CF_{234} to CF_{123}, thus forming a connected set.

Theorem 1 *Let q_s and q_g be two configurations in free configuration space and $H(q_s)$ and $H(q_g)$ be the accessed configuration on convex-HGVG for q_s and q_g respectively. Then, there is a path between q_s and q_g, if and only if there exists a path between $H(q_s)$ and $H(q_g)$ that lies entirely on convex-HGVG.*

To prove this theorem, we need following Lemmas. The central part of the proof is to show that R-edges connect two convex-GVG edges associated with two adjacent junction regions, which can be stated more formally as follows.

Lemma 1 *Let q_1 be a configuration in CF_{ijk} and q_2 be a configuration CF_{ijl}. If there exists a path $s(t)$ between them, then there exists a R-edge R_{ij} that connects CF_{ijk} and CF_{ijl}, and therefore there is a path between $H(q_1)$ and $H(q_2)$ which lies on convex-HGVG (where $H(q_1)$ and $H(q_2)$ represent the accessed configuration on convex-HGVG for q_1 and q_2 respectively).*

Before we prove Lemma 1, we introduce additional geometry. Note that any path that connects two convex-GVG edges must "pass through" the line segment $c_i^* c_j^*$, where c_i^* and c_j^* are the closest pair of points in C_i and C_j respectively. To maximize the minimum distance along such a path, the robot must align itself so that its "principal axis" is normal to the vector $c_i^* - c_j^*$, i.e. parallel to the $T_{c_i^*} C_i$ and $T_{c_j^*} C_j$ (Fig. 7). By the definition of an R-edge, this configuraion m^* lies on an R-edge. Such a configuration m^* is actually a saddle point of the distance on CF_{ij}. Also, for any path on CF_{ij} that connects CF_{ijk} and CF_{ijl}, the minimum distance is smaller than $D(m^*)$.

To prove the Lemma 1, we will need the following Lemma.

Lemma 2 *Given a principal axis v_k, a distance $\delta > D(m^*)$, there are four configurations that satisfy the R-edge condition, i.e., there are four configurations q such that (i) $D_i(q) = D_j(q) = \delta$, (ii) $\langle c_i(q) - c_j(q), v_k \rangle = 0$.*

Proof: Note that there are two R-edges associated with C_i and C_j and the given principal axis v_k, and as the robot travels along the R-edges, there will be two configurations on each of these two R-edges, that satisfies $D_i(q) = D_j(q) = \delta$. In the following proof, we show that there is one configuration on one "side" of the *one* R-edge that satisfies the conditions specified in the statement above. We show this by contradiction. From now on, we consider the expanded robot by δ. Thus, $r_i(q) = c_i(q)$ and $r_j(q) = c_j(q)$ for this expanded robot. Note that for the extended shape, c_i and c_j do not changes and the v_k is still a principal axis. Let b_k and t_k be the top and bottom point associated with the given principal axis v_k and let c_i^* and c_j^* be the closest points on C_i and C_j. Also let $\phi_i(q)$ be the angle between the vector $c_i(q) - c_j(q)$ and the tangent of the robot boundary at point $c_i(q)$.

Now, assume that there are two configurations q_1 and q_2 on CF_{ij} such that $D_i(q_1) = D_i(q_2) = \delta$ and $\langle c_i(q_1) - c_j(q_1), v_k \rangle = 0$ and $\langle c_i(q_2) - c_j(q_2), v_k \rangle = 0$. This implies that $c_i(q_1) - c_j(q_1)$ and $c_i(q_2) - c_j(q_2)$ are both parallel to the vector $t_k - b_k$. Since the robot is convex, $|c_i(q_1) - c_j(q_1)| \neq |c_i(q_2) - c_j(q_2)|$ if $q_1 \neq q_2$. Assume, without loss of generality, $|c_i(q_1) - c_j(q_1)| > |c_i(q_2) - c_j(q_2)|$. This implies that the vector $c_i(q_1) - c_j(q_1)$ is closer to the vector $t_k - b_k$ than $c_i(q_2) - c_j(q_2)$, and in turn, this implies that $\phi_i(q_1) > \phi_i(q_2)$ and $\phi_j(q_1) > \phi_j(q_2)$ (Figs. 10, 11).

Now we consider the locations of c_i and c_j on the boundary of the obstacles. Note that at c_i the tangents of the robot boundary and the obstacle boundary coincide. Therefore $\phi_i(q)$ is also the angle between the vector $c_i(q) - c_j(q)$ and the tangent of the obstacle boundary at point $c_i(q)$. There can be three possibilities: (i) $c_i(q_1) = c_i(q_2)$, (ii) $c_i(q_2)$ gets closer to c_i^* than $c_i(q_1)$ and (iii) $c_i(q_2)$ gets farther from c_i^* than $c_i(q_1)$. For the case (i) and (iii), from the assumption, $c_j(q_2)$ must be closer to c_j^* than $c_j(q_1)$ (otherwise, from the convexity of the obstacles, $|c_i(q_1) - c_j(q_1)| < |c_i(q_2) - c_j(q_2)|$. This results $\phi_j(q_2) > \phi_j(q_i)$, which is a contradiction. For case (ii), again from the convexity of the obstacles, $\phi_i(q_2) + \phi_j(q_2) > \phi_i(q_1) + \phi_j(q_1)$, which is also a contradiction. Therefore, there can be only one configuration that satisfies the R-edge condition given δ on one "side" of the R-edge. ∎

Now we prove Lemma 1.

Proof: From the observation above, there is a saddle point m^* on CF_{ij} if there is a path between CF_{ijk} and CF_{ijl}, and m^* is in R_{ij}. We now show that we can grow the R-edge from m^* to both directions as we increases the distance from the obstacles. First, take a small neighborhood $B(m^*)$, then since R_{ij} is 1-manifold, it contains some configurations in R_{ij} and since the m^* is a saddle point, and there is only unique configuration with distance $D_i(m^*)$ on R_{ij} (Lemma 2), there must be a configuration q_1 in $B(m^*)$ with $D_i(q_1) > D_i(m^*)$. Now take a neighborhood $B(q_1)$ of q_1. then, using similar argument, it contains a configuration q_2 such that $D_i(q_2) > D_i(q_1)$. Therefore, the distance to closest obstacles monotonically increases as the robot moves away from the saddle point m^*, and since the environment is bounded, the R-edge R_{ij} terminates at a three-way equidistant configuration. ∎

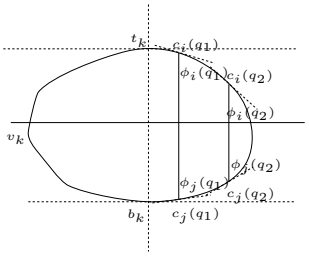

Figure 10: If q_1 and q_2 both satisfies the R-edge condition, $c_i(q_1) - c_j(q_1)$ and $c_i(q_2) - c_j(q_2)$ are parallel to each other, and from the convexity of the robot $|c_i(q_1) - c_j(q_1)| \neq |c_i(q_2) - c_j(q_2)|$. $\phi_i(q)$ is the angle between $c_i(q) - c_j(q)$ and the $t_k - b_k$. Note that if $|c_i(q_1) - c_j(q_1)| > |c_i(q_2) - c_j(q_2)|$, $\phi_i(q_1) > \phi_i(q_2)$.

Finally we prove Theorem 1.

Proof: If there is a path between $H(q_s)$ and $H(q_g)$, which lies entirely on convex-HGVG, then it is obvious that there exists a path between q_s and q_g since there exist paths between q_s and $H(q_s)$ and between q_g and $H(q_g)$, from accessibility.

Now, assume there exists a path $c(t)$ between q_s and q_g, i.e., $c \in C^0$, $c(0) = q_s$, $c(1) = q_g$ and $c(t)$ is in free configuration space for all $t \in [0, 1]$. Let's denote q_s as q_0 and q_g as q_{n+1}, and let J_0 and J_{n+1} be the junction regions that contain q_0 and q_{n+1} respectively. Also, J_0, J_1, J_2, ... J_n, J_{n+1} be the sequence of the junction regions that the path $c(t)$ passes through. Then J_i and J_{i+1} (for $i = 0$ to n) are adjacent to each other. Let q_i be a configuration on $c(t)$ which is contained in the junction region J_i, and let $H(q_i)$ be the accessed configuration on convex-HGVG for q_i. Then, since J_i and J_{i+1} are adjacent to each other, from Lemma 1, there exists a path between $H(q_i)$ and $H(q_{i+1})$. which lies on convex-HGVG. This implies there exits a path between $H(q_s)$ and $H(q_g)$ on convex-HGVG, which is a concatenation of the paths between $H(q_i)$ and $H(q_{i+1})$ for $i = 0$ to n. ∎

4 Control Laws and Incremental Construction Method

The control laws for construction of the convex-HGVG is a simple adaptation for the point based GVG approach. For generating a convex GVG-edge, the planner uses a control

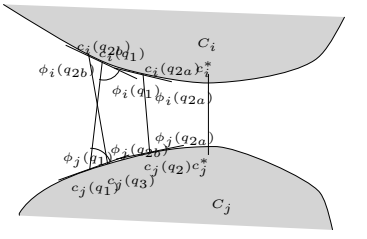

Figure 11: Changes of Locations of c_i, c_j and Φ_i and Φ_j as viewed on the obstacle boundaries.

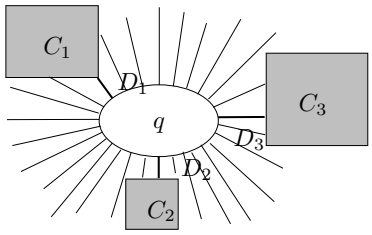

Figure 12: The distance to a obstacle is the local minima of the distance given by range sensors around the perimeter of the robot.

law that traces the roots of the expression

$$G(q) = \begin{bmatrix} D_i(q) - D_j(q) \\ D_i(q) - D_k(q) \end{bmatrix} \quad (5)$$

according to the control law

$$\dot{q} = \alpha \text{Null}(\nabla G(q)) + \beta(\nabla G(q))^{\dagger} G(q), \quad (6)$$

where

- α and β are scalar gains,
- ∇G is the gradient of G,
- $\text{Null}(\nabla G(q))$ is the null space of $\nabla G(q)$,
- $(\nabla G(q))^{\dagger}$ is the Penrose pseudo inverse of $\nabla G(q)$, i.e.,

$$(\nabla G(q))^{\dagger} = (\nabla G(q))^{T} (\nabla G(q)(\nabla G(q))^{T})^{-1}. \quad (7)$$

To invoke the control law in Equation 6, the robot needs only distance information. For the moment, assume that the robot has a ring of range sensors, such as a laser ranger or a sonar ring, deployed around its perimeter. Local minima of this array correspond to distance to nearby obstacles. (Figure 12)

Finally, the R-edges can be constructed using the same control law by tracing the root of the expression

$$G(q) = \begin{bmatrix} D_i(q) - D_j(q) \\ v_s \cdot (c_i - c_j) \end{bmatrix}. \quad (8)$$

5 Simulation

Figure 13 shows the swept volume of the convex-GVG edges for a non-symmetric convex robot. As noted before, the convex-GVG edges themselves are not connected. Figure 14 shows the swept volume of the convex-R-edge in the same environment, and Figure 15 shows the swept volume of convex-HGVG.

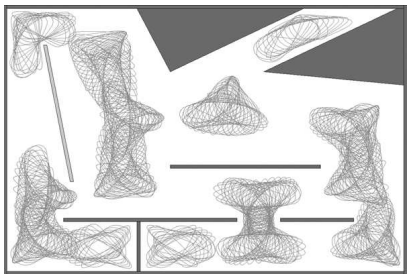

Figure 13: The convex-HGVG : The placements of the robot along the convex-GVG edges

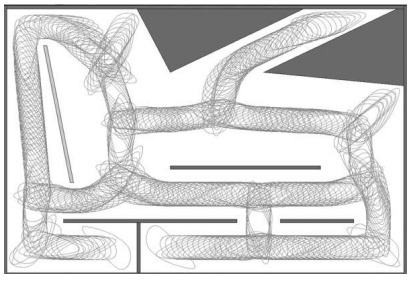

Figure 14: The convex-HGVG : The placements of the robot along convex-R-edges

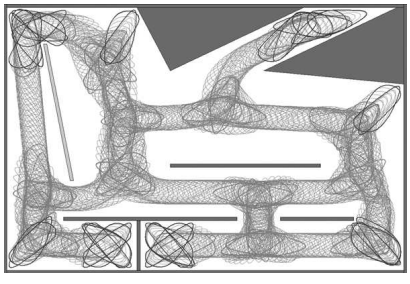

Figure 15: The convex-HGVG : The placements of the robot along the convex-HGVG

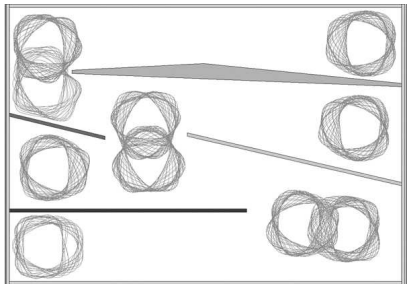

Figure 16: The convex-HGVG : The placements of the robot along the convex-GVG edges

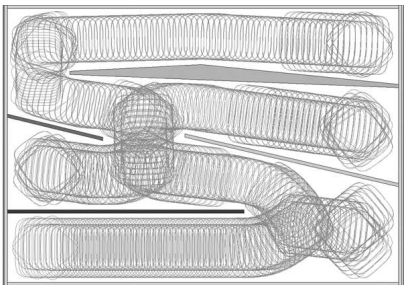

Figure 17: The convex-HGVG : The placements of the robot along the convex-R-edges

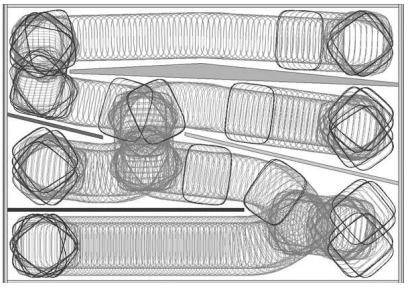

Figure 18: The convex-HGVG : The placements of the robot along the convex-HGVG

Figures 16, 17 and 18 show another example of the convex-HGVG. In this example, the robot has the rectangular shape with round corner, and symmetric about two axes which are normal to each other. These symmetric axes are also principal axes. Therefore, there can be two different R-edges that connect two disconnected GVG-edges Note that in the lower left corner of the room there is disconnected components of a GVG-edge and two R-edges connects these disconnected components to the GVG-edge on the lower right corner of the room.

6 Conclusion

This paper introduces a new roadmap called *convex hierarchical generalized Voronoi graph* for a convex body operating in a two dimensional workspace. The convex-HGVG is defined in terms of workspace distance information which is within line of sight of the robot and thus can be implemented in a sensor-based way. The convex-HGVG comprises two component components : (i) convex-GVG edges, which are three-way equidistant, (ii) R-edges, which are two-way equidistant, and connect disconnected convex-GVG edges. This definition is a result of not being able to contract $SE(2)$, with arbitrary holes removed from it, onto a one-dimensional set. Instead, we break down $SE(2)$ into contractible regions, each having its own convex-GVG, and connect the regions with R-edges. What is interesting here is that R-edges are essentially a topological representation of the workspace, but we are using them to infer topological properties of the configuration space.

Since this roadmap is defined in terms of workspace distance information, we can prescribe a sensor-based incremental method to achieve motion planning without constructing the configuration space. This is important for sensor based planning because we cannot construct configuration space without knowing the workspace first. Moreover, even when we have configuration space representation, it is still difficult to measure the distance in configuration space than in workspace. Finally we show some simulation result for convex-HGVG in sample environments.

This work is a step towards the ultimate goal of sensor based planning for an articulated multi-body robot. The next steps are to define a roadmap for convex body operating in three-dimensional workspace and two-convex-body operating in two/three dimensional workspace.

References

[1] J.F. Canny. *The Complexity of Robot Motion Planning.* MIT Press, Cambridge, MA, 1988.

[2] H. Choset and J. Burdick. Sensor Based Motion Planning: Incremental Construction of the Hierarchical Generalized Voronoi Graph. *International Journal of Robotics Research*, 19(2):126–148, February 2000.

[3] H. Choset and J. Burdick. Sensor Based Motion Planning: The Hierarchical Generalized Voronoi Graph. *International Journal of Robotics Research*, 19(2):96–125, February 2000.

[4] Howie Choset and Ji Yeong Lee. Sensor-Based Construction of a Retract-Like Structure for a Planar Rod Robot. *IEEE Transaction of Robotics and Automation*, 17, 2001.

[5] J. Cox and C.K. Yap. On-line Motion Planning: Case of a Planar Rod. In *Annals of Mathematics and Artificial Intelligence*, volume 3, pages 1–20, 1991.

[6] S.S. Keerthi, C.J. Ong, E. Huang, and E.G. Gilbert. Equidistance diagram- A new roadmap for path planning. In *Proceedings of the IEEE Conference on Robotics and Automation*, pages 682–687, May 2000.

[7] Ji Yeong Lee, Howie Choset, and Alfred A. Rizzi. Sensor Based Planning for Rod Shaped Robots in Three Dimensions: Piece-wise Retracts of $\mathbb{R}^3 \times S^2$. In *Proceedings of IEEE International Conferenec on Robotics and Automation*, pages 991 –999, May 2001.

[8] V. Lumelsky and A. Stepanov. Path Planning Strategies for Point Mobile Automaton Moving Amidst Unknown Obstacles of Arbitrary Shape. *Algorithmica*, 2:403–430, 1987.

[9] C. Ó'Dúnlaing and C.K. Yap. A "Retraction" Method for Planning the Motion of a Disc. *Algorithmica*, 6:104–111, 1985.

[10] N.S.V. Rao, S. Kareti, W. Shi, and S.S. Iyenagar. Robot Navigation in Unknown Terrains: Introductory Survey of Non-Heuristic Algorithms. *Oak Ridge National Laboratory Technical Report*, ORNL/TM-12410:1–58, July 1993.